UCRL-CONF-230835

High-Energy Neutron Imaging Development at LLNL

J. M. Hall (PI), B. Rusnak and P. J. Fitsos

Lawrence Livermore National Laboratory

7 May 2007

Published in *Proc. of 8th World Conference on Neutron Radiography* (Gaithersburg, MD, 2006)

Disclaimer

Auspices Statement

This work was performed under the auspices of the U. S. Department of Energy (DOE) by the University of California, Lawrence Livermore National Laboratory (LLNL) under Contract No. W-7405-Eng-48.

HIGH-ENERGY NEUTRON IMAGING DEVELOPMENT AT LLNL

J. Hall, B. Rusnak and P. Fitsos

Lawrence Livermore National Laboratory, Livermore, CA 94550-9900

*Corresponding author E-mail: *jmhall@llnl.gov*

Abstract. LLNL is currently engaged in the development of high-energy (10 MeV) neutron imaging technology to complement existing x-ray diagnostic tools in U.S. Department of Energy (DOE) nondestructive evaluation (NDE) applications. Our goal is to develop and deploy a nonintrusive imaging system capable of detecting cubic-mm-scale voids, cracks or other significant structural defects in heavily-shielded low-Z materials within very thick objects. The final production-line system that we envision will be relatively compact (suitable for use in existing facilities within the DOE complex) and capable of acquiring both radiographic and tomographic (CT) images. In this paper, the design status of the high-intensity, accelerator-driven neutron source and large-format imaging detector associated with the system will be discussed and results from one recent neutron imaging experiment conducted at the Ohio University Accelerator Laboratory (OUAL) in Athens, OH will be presented.

INTRODUCTION

We are proceeding with the development of a high-energy (10 MeV) neutron imaging system for use as an inspection tool in U.S. Department of Energy (DOE) nondestructive evaluation (NDE) applications. Our goal is to develop and deploy a nonintrusive imaging system capable of detecting cubic-mm-scale voids, cracks or other significant structural defects in heavily-shielded low-Z materials within very thick objects (*e.g.* $\rho x > 100$ gm/cm^2). Due to the better penetration of neutrons through high-Z materials and their higher interaction cross sections in low-Z materials, we believe that high-energy neutron imaging will be capable of detecting structure in thick objects which may be essentially opaque to conventional x-ray systems; however, we would like to emphasize that our intent here is to develop an inspection system that will *complement* - not replace - existing or proposed DOE NDE x-ray diagnostic tools.

The final production-line imaging system that we envision will be relatively compact (suitable for use in existing or proposed inspection facilities within the DOE complex) and capable of acquiring both radiographic and tomographic (CT) images of objects under inspection. It will consist of an intense, accelerator-driven D(d,n)^{3}He neutron source ($E_n \sim 10$ MeV @ 0°) with an effective yield of $\sim 10^{11}$ n/sec/sr along the beam axis and a focal spot size of ≤ 1.50 mm (FWHM), a multi-axis rotation/translation stage to support and manipulate objects and a neutron imaging detector. The imaging detector itself will consist of a simple transparent plastic scintillator (*e.g.* BC-400 or

BC-408) viewed indirectly by a single large-format CCD camera located in a well-shielded environment out of the direct beam path. The geometric magnification factor of the system will likely be ~ 1.25:1 and its ultimate spatial resolution should be ≤ 1.00 mm (FWHM) at the object position.

The conceptual design of the proposed imaging system and results from a wide variety of neutron imaging experiments conducted at the Ohio University Accelerator Laboratory (OUAL) in Athens, OH, over the past few years using a relatively simple prototype imaging detector have already been published in the open literature [1 - 6] or documented in open-source LLNL internal reports. In this paper, the design status of the high-intensity, accelerator-driven neutron source and large-format imaging detector associated with the system will be discussed and results from one recent neutron imaging experiment conducted at OUAL will be presented.

1. NEUTRON SOURCE DEVELOPMENT

The accelerator system that we propose to use in our full-scale neutron source will be based on mature, commercially-available technology. It will consist of a D^+ ion source and a pair of compact radio-frequency quadrupoles (RFQs) coupled to a short drift-tube linac (DTL). The system will accelerate D^+ ions to an energy of ~ 7 MeV and be capable of delivering an average ion current of ~ 325 μA to a D_2 gas cell located in a target endstation. The beam pulse frequency will be ~ 140 Hz and the duty factor will be ~ 1.95% (this implies a peak current of ~ 15 - 17 mA and a pulse width of ~ 139 μsec). The beam emittance ($\varepsilon_{x,y}$) will be held to ≤ 4 π mm-mrad in order to achieve the small focal spot size required for imaging.

The full-up engineering design for this accelerator system was completed by AccSys Technologies, Inc. in late 2002; however, its procurement has been repeatedly delayed due to funding restrictions (projected cost ~ $2.9M). In the mean time (a post-WCNR8 development), we have recently acquired a smaller (4 MeV) RFQ capable of delivering an average D^+ ion current of ~ 100 μA with essentially the same beam structure. This system, which is currently being decommissioned by another project at LLNL, will be re-commissioned in the laboratory's well-shielded accelerator facility during late 2007 and should be available for use in neutron source technology assessment and imaging experiments (E_n ~ 7 MeV @ 0°) by early 2008.

The simultaneous requirements for a large average D^+ ion current (~ 325 μA) and a relatively small focal spot size (≤ 1.50 mm (FWHM)) imposed by our proposed imaging application effectively preclude the use of a conventional (*i.e.* "windowed") D_2 gas cell in our target endstation due to the fact that there simply exist no window materials capable of handling the extremely large areal power densities that we anticipate with our source (*e.g.* ~ 130 kW/cm^2 (average), ~ 6600 kW/cm^2 (peak)); therefore, we have focused our effort thus far on the development of "windowless" D_2 gas cell designs which can be incorporated into an endstation and coupled to our pulsed-beam accelerator system for use as an intense neutron source.

One of the most promising ways to deal with large average or peak areal power densities is to use a "rotating-aperture" (RA) gas cell design. In this type of system, narrow (~ 4 - 5 mm Ø) entrance and exit apertures on the high-pressure (~ 3 atma) gas cell (and any adjacent differential pumping stages) are "open" only when they happen to coincide with matching apertures in a series of rotating disks synchronized to the pulse frequency of the accelerator beam. This effectively isolates the high-pressure gas in the cell from the accelerator vacuum system. Pioneering research at MIT [7 - 10] demonstrated that even a rudimentary RA system can create a very effective "plug" between a pressurized gas cell and a differential pumping system and work done at an industrial laboratory in South Africa [11] has since proven the effectiveness of RA systems in production-line imaging applications.

We have developed a (3rd generation) multi-stage RA gas cell design is that utilizes a 4-cm-wide cross-flow D_2 venturi capped at either end by 5-mm Ø rotating apertures (*cf.* Figure 1). With a venturi capable of generating very high flow rates (*e.g.* ~ 200 - 400 m/s), the D_2 gas in the beam channel (≤ 1.50 mm (FWHM)) can be effectively refreshed ≥ 20 times during the course of a single beam pulse (~ 139 μsec), thereby mitigating potential density rarefactions in the gas due to beam heating (*i.e.* "burn through") and the attendant decrease in neutron yield that one might normally expect for a given incident beam current and gas cell pressure. Detailed ALE3D gas hydrodynamic calculations done at LLNL confirmed that it should be possible to maintain a D_2 gas density in the beam channel equivalent to an average pressure of ~ 3 atma using this approach. This, in turn, should allow us to generate average neutron yields which are ~ 90% (or better) of the desired level.

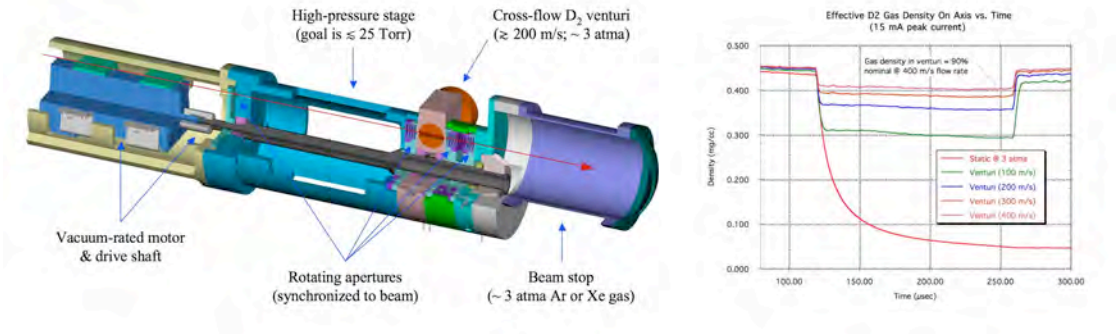

FIGURE 1. Cutaway drawing from engineering design for 3rd generation RA endstation and plot of predicted effective D_2 gas density on axis vs. time (based on ALE3D calculations).

After the incident D^+ ion beam passes through the D_2 gas cell in the endstation, its residual energy needs to be dissipated in a way that not only has minimal impact on the intensity and spatial distribution of the primary (quasi-monoenergetic) neutron beam generated in the gas cell, but which also produces as few additional (broad-spectrum) neutrons as possible. Our current intent is to dump the beam into a high-pressure (~ 3 atma), high-Z gas such as Ar or Xe located immediately downstream from the D_2 gas cell. The incident beam power (~ 2.28 kW (average)) could then be removed by using a heat exchanger in the high-Z gas recirculation loop. Our calculations indicate that the rotating aperture doublet located at the exit of the target gas cell in our 3rd genera-

tion design should serve to minimize mixing between the two gases (the purity of the different gas streams could also potentially be maintained by using a gas handling system that exploits differences in the thermodynamic transport properties of the gases). High-pressure Ar or Xe gas should have essentially no impact on either the intensity or the spatial distribution of the primary neutron beam and beam breakup measurements for D^+ ions incident on Ar and Xe have shown that neither produces a significant number of additional (broad-spectrum) neutrons at the D^+ ion energies of interest here; however, additional ALE3D gas hydrodynamics calculations will be done to ensure that beam "burn through" in the stopping gas and turbulent mixing between the target and stopping gases will not pose problems.

Based on bench tests of a full-scale prototype, we are reasonably confident that our 3rd generation RA endstation design will serve our purposes; however, we are also developing a much more facility-friendly "pulsed gas injection" system in which D_2 gas is pressurized via natural dynamic flow processes in the gas handling system and then injected into the target gas cell using a pneumatically-actuated valve assembly only when the beam is present (*cf.* Figure 2). The high-Z Ar or Xe gas used as a beam stop would be handled using the same technique. This sort of system (which does not involve the use of rotating apertures to cap the gas cell) is *also* very well suited for use with a pulsed-beam accelerator such as our proposed RFQ/DTL system *and*, based on our design calculations, it should be able to meet our target gas density requirements (*i.e.* ~ 3 atma equivalent during the beam pulse) with D_2 gas volumes and pumps which are an order of magnitude or more smaller than those required for our RA gas cell. A full-scale prototype of this system is currently being designed and will be field-tested with our small (4 MeV) RFQ accelerator in early 2008.

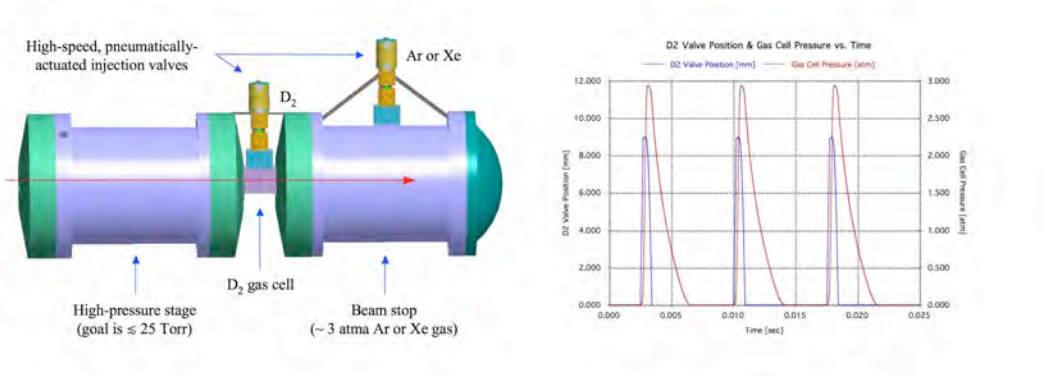

FIGURE 2. Solid model drawing from engineering design for proposed "pulsed gas injection" endstation and plot of predicted D_2 valve motion and corresponding gas cell pressure vs. time.

2. IMAGING DETECTOR DEVELOPMENT

The development of a high-efficiency, large-format neutron detector suitable for use in a full-scale, production-line imaging system is also critical to the success of this project. While the prototype detector developed for use in our experiments at OUAL has worked quite well thus far, allowing us to validate the potential of neutron imaging by capturing radiographic and tomographic images of a variety of test objects, its field of view (FOV) is only ~ 30 cm X 30 cm. We estimate that a full-scale imaging detector

will need to have a useful FOV ≥ 2 times this size in order to meet the requirements of potential DOE production-line NDE applications.

Our full-scale prototype of the detector (*cf.* Figure 3) will consist of a ~ 2 – 4 cm thick, 65 cm X 65 cm plastic scintillator (*e.g.* BC-400 or BC-408) viewed by a single large-format CCD camera. A thin (~ 0.125") turning mirror with an aluminized front surface will be used to redirect light from the scintillator into the camera, thereby allowing it to be located off axis in a relatively well-shielded environment out of the direct neutron beam path. The detector system will be mounted on a single 4' X 5' optical table and enclosed in a light-tight aluminum housing.

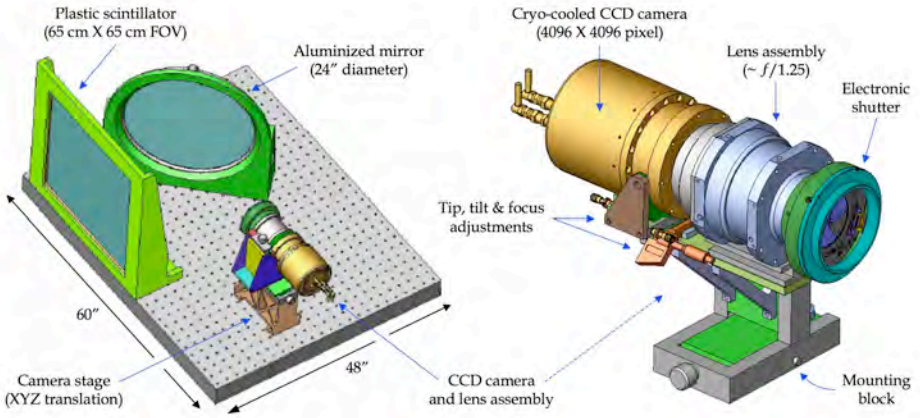

FIGURE 3. Engineering drawings showing layout for full-scale prototype of neutron imaging detector. The entire assembly will be enclosed in a light-tight aluminum housing (not shown).

The custom lens assembly that will be used in the detector (built by Optics1, Inc. of Westlake Village, CA) has been designed to provide high light collection efficiency (~ *f*/1.25) and uniform focus over the full 65 cm X 65 cm FOV at the scintillator. A UniBlitz® high-speed, large-aperture (90-mm) electronic shutter will be used to prevent stray light from entering the lens between image frames.

The CCD camera that will be used (built by Spectral Instruments, Inc. of Tucson, AZ) features a Fairchild 4096 X 4096 (15 μm) pixel, back-illuminated sensor with a "UV-enhanced" anti-reflective coating optimized for BC-400 / BC-408 spectral sensitivity. It has a 4-port parallel readout system with 16-bit digitization and the sensor can be cryogenically cooled to ~ -100 ˚C, which will effectively eliminate thermal noise and enable long (~ 1 hr) integration times if needed. It should be noted that, since the ultimate spatial resolution of an imaging detector such as this is usually limited by either source spot size or the intrinsic resolution of the scintillator, we will not necessarily be able to take advantage of the resolving power that would normally afforded by a 4096 X 4096 chip (*e.g.* we will likely opt to use on-chip binning to improve pixel counting statistics by imaging at ~ 1024 X 1024 instead); however, this particular sensor was chosen because its physical size (61.45 mm X 61.45 mm) *significantly* enhances the camera's sensitivity when imaging a large FOV such we have here.

The key components of this imaging detector are currently in hand or in fabrication at LLNL. The full-scale prototype will be assembled and bench-tested during the fall of 2007 and should be ready for use in imaging experiments at LLNL when our small RFQ-driven neutron source comes online in early 2008.

3. RECENT IMAGING EXPERIMENTS

We have conducted high-energy neutron imaging experiments on more than 25 different test objects over the course of the past few years at OUAL using a relatively simple prototype imaging detector (described below). The test objects typically consisted of low-Z materials (*e.g.* polyethylene, ceramics, *etc.*) sandwiched between high-Z materials (*e.g.* lead, tungsten, etc.) for radiographic imaging experiments and multi-layer (high-Z / low-Z) cylindrical assemblies for tomographic imaging experiments. Each of these objects was designed to simulate one or more hypothetical structural defects in systems of interest to the DOE. Our basic experimental procedures at OUAL and one recent set of results will be described here.

A nearly monoenergetic, 10 MeV neutron beam was generated by focusing 6.85 MeV D^+ ions extracted from OUAL's tandem van de Graaff accelerator into a cylindrical D_2 gas cell, 1 cm in diameter and ~ 8 cm long, attached to the end of a beam line. The gas cell was capped with a thin (~ 5 μm) W entrance window and maintained at a static pressure of ~ 45 psia (~ 3 atma). The average D^+ ion current at the gas cell was ~ 8.5 μA during each of the imaging runs. This corresponds to an estimated 10 MeV neutron yield of ~ 5.6×10^9 n/sec/sr along the beam axis (*i.e.* ~ 5% of the intensity of the source proposed for our full-scale system). The effective focal spot size of the beam at OUAL was ~ 3 mm (FWHM) at the entrance window to the gas cell (*i.e.* ~ 2X that of the source proposed for our full-scale system). The test objects were placed on a rotation stage ~ 200 cm from the neutron source and ~ 200 cm from the imaging detector, resulting in a geometric magnification factor of ~ 2:1 at the image plane. The imaging detector consisted of a 30 cm X 30 cm X 4 cm thick BC-408 transparent plastic scintillator viewed indirectly by a single 1024 X 1024 (24 μm) pixel, LN_2-cooled, CCD camera with a high-speed (f/1.0) commercial photographic lens.

Tomographic (CT) imaging of test objects was done using a high-precision, computer-controlled rotation stage interfaced to our data acquisition system. The control system (driven by a simple LabView script) is fully automated, virtually immune to neutron source faults (*i.e.* temporary or even long-term loss of beam) and capable of taking CT data sets consisting of 4, 8, 16, 32, 64, 128, *etc.* interleaved images of an object at equally spaced angular intervals distributed over a 360º rotation.

The test object that we will report on here consisted of a 4.00" high, 2.00" Ø polyethylene cylinder shielded by a 1.00" thick lead shell and a 0.50" thick aluminum sleeve (*cf.* Figure 4). The poly cylinder actually consisted of two "half cylinders" with a series of 11 holes ranging in diameter from 10.00 mm down to ~ 0.40 mm machined into the inner (flat) surface of one half and the outer (curved) surface of the other. The maximum value of ρx for this object (measured along the inner radius of the Pb shell)

was estimated to be ~ 107 gm/cm^2. The assembly was mounted on a low-mass aluminum stand attached to the rotation stage and imaged perpendicular to its principal axis. The full neutron CT data set in this case consisted of a series of 128 20 minute exposures taken over a 360˚ rotation ($\Delta\theta$ = 2.8125˚). To our good fortune, this particular test object was *also* recently imaged by LLNL's x-ray imaging team using the laboratory's high-intensity 9 MeV x-ray imaging system [12], thereby providing us with a convenient "benchmark" for comparing neutron and x-ray image quality for relatively thick objects. The full 9 MeV x-ray CT data set consisted of a series of 900 20 second exposures taken over a 360˚ rotation ($\Delta\theta$ = 0.4000˚).

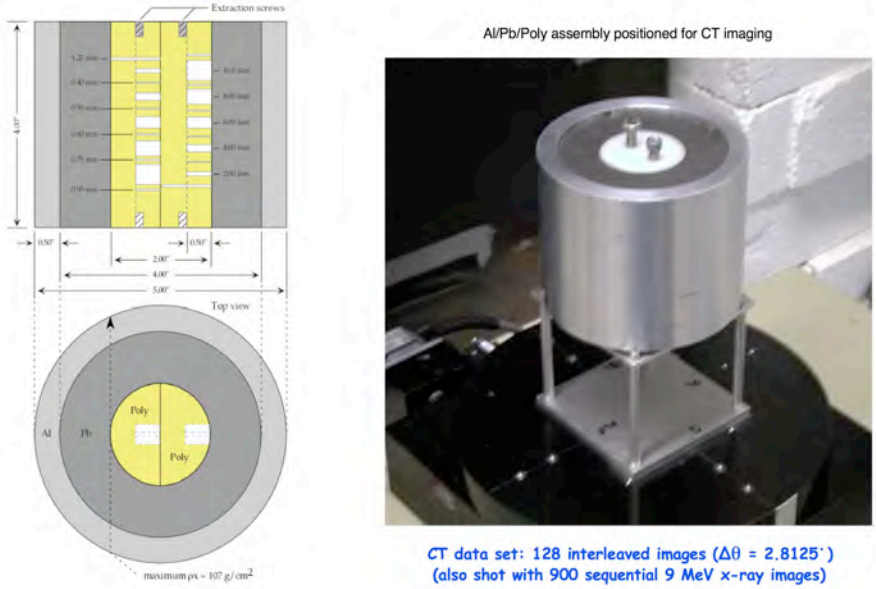

FIGURE 4. Test object used in neutron tomographic (CT) imaging experiments conducted at OUAL and recent 9 MeV x-ray CT imaging experiments conducted at LLNL.

Individual radiographic images extracted from the 10 MeV neutron and 9 MeV x-ray CT data sets at similar viewing angles (0˚) each revealed the basic structure of the test object (*cf.* Figure 5); however, the neutron images showed significantly higher contrast and revealed much more structural detail (*e.g.* the narrow (≤ 0.005") "contact gap" between the two halves of the poly cylinder) than did the x-ray images. The shell structure of the test object and voids in the poly cylinder as small as ~ 1.25 mm in diameter were clearly discernable in vertical slices taken at 0˚ through the neutron CT reconstruction (*cf.* Figure 6). The larger voids (≥ 1.25 mm Ø) near the center of the poly cylinder were also clearly discernable in vertical slices taken at 90˚ through both the neutron and x-ray CT reconstructions (*cf.* Figure 7); however, the neutron images again showed much higher contrast, allowing the full structure of the test object (*e.g.* voids *and* inner surface contours) to be viewed at a single contrast setting. Horizontal slices taken through the neutron CT reconstruction at various elevations clearly revealed both the void structures in the test object and the narrow contact gap between the two halves of the poly cylinder (*cf.* Figure 8). The void structures and contact gap were *also* discernable in the x-ray CT reconstruction, although (again) at a *much* lower contrast level. In fairness, we should note that the spatial resolution in the x-ray image

is superior. This is not entirely unexpected due to a combination of factors including the smaller spot size of the LLNL x-ray source (~ 1 mm (FWHM)), a smaller geometric magnification factor (~ 1.2:1) and the higher intrinsic resolving power of the specialized glass scintillators typically used for x-ray imaging.

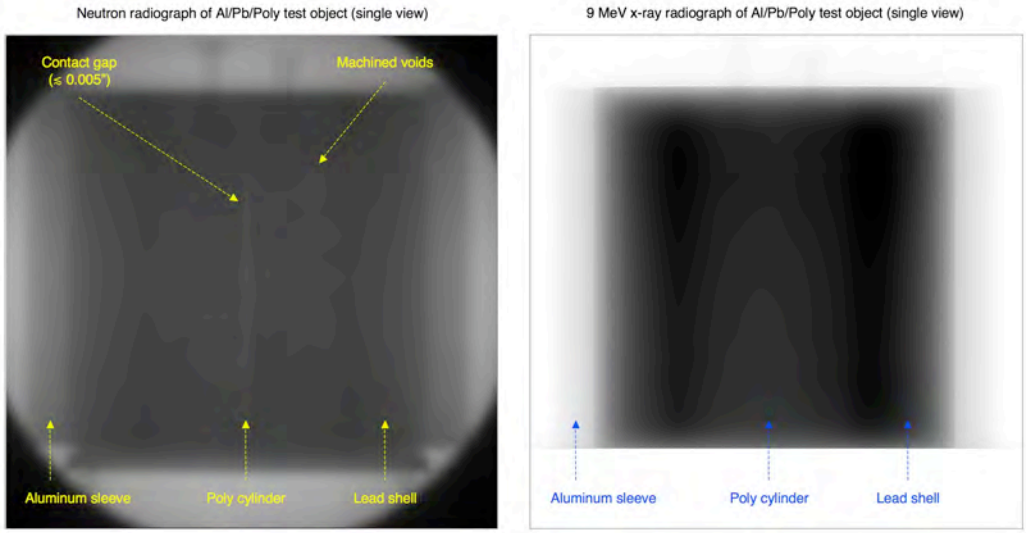

FIGURE 5. Individual radiographic images extracted from the 10 MeV neutron (left) and 9 MeV x-ray (right) CT data sets at similar viewing angles (0˚ in this case). The basic structure of the object was discernable in both cases; however, the individual neutron images showed significantly higher contrast and revealed much more structural detail than did the individual x-ray images.

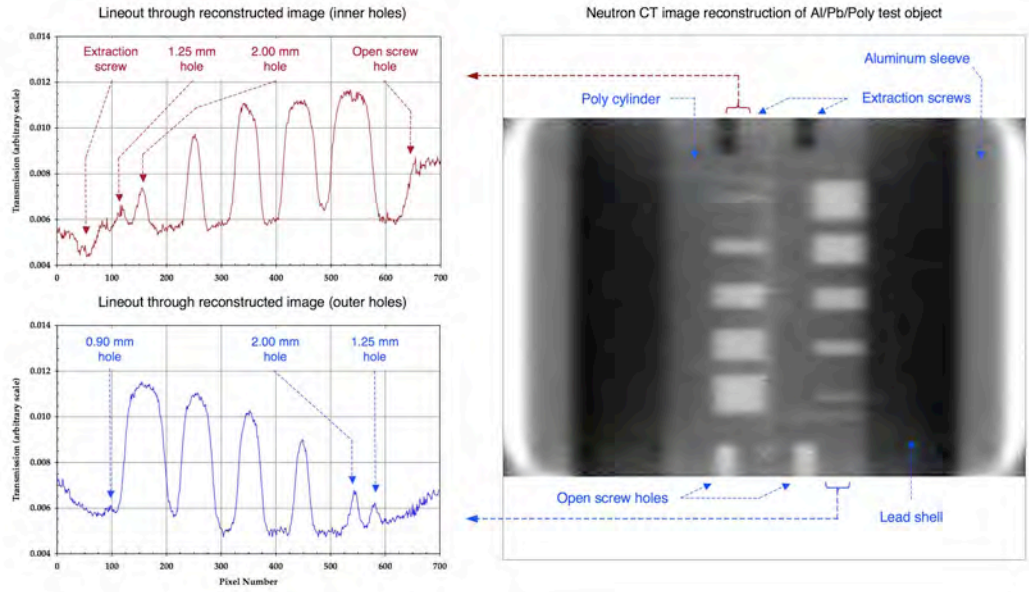

FIGURE 6. Neutron CT reconstruction of test object (vertical slice at 0˚ viewing angle) and lineouts taken through the reconstruction at two locations. The detailed structure of the object (*e.g.* outer *and* inner material contours, extraction screws, open screw holes and voids in the poly cylinder as small as ~ 1.25 mm in diameter) was clearly discernable in the reconstruction and / or lineouts.

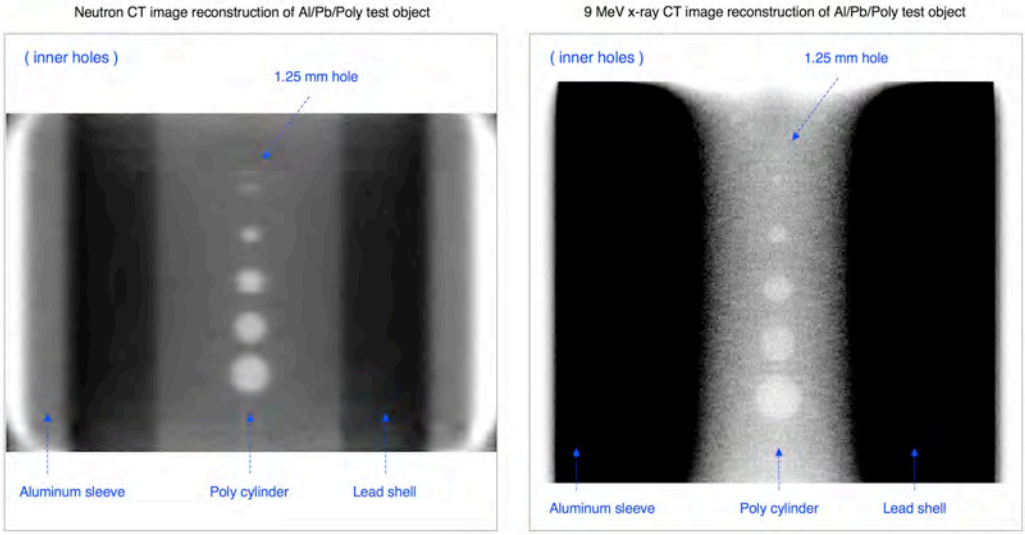

FIGURE 7. Comparison of 10 MeV neutron (left) and 9 MeV x-ray (right) CT reconstructions of test object (off-axis vertical slices through inner hole set at 90° viewing angle). Note that the full structure of the test object (*e.g.* voids *and* material contours) can be viewed at a single contrast setting in the neutron CT, whereas the contrast in the x-ray image had to be adjusted down to the bottom 3% of its range to make the void structures visible in this case.

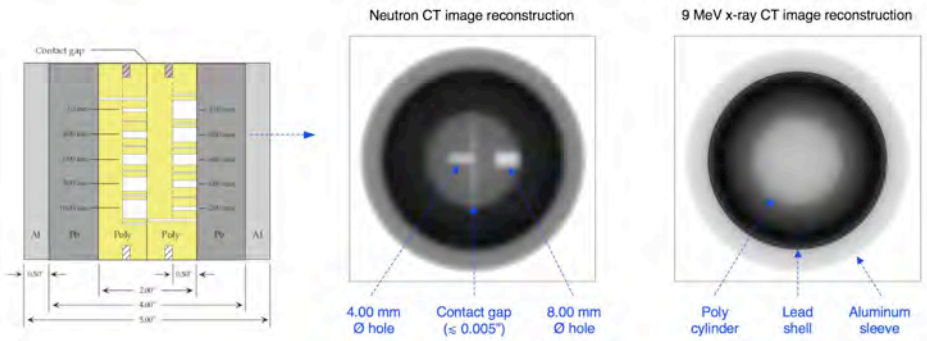

FIGURE 8. Comparison of 10 MeV neutron (left) and 9 MeV x-ray (right) CT reconstructions of test object (horizontal slices through 4.00 / 8.00 mm Ø hole set). Both images are shown at full contrast range in this case. The superior spatial resolution in the x-ray image is due to a combination of factors related to the physics of x-ray imaging and the implementation of LLNL's system.

CONCLUSIONS

We believe that the wide variety of neutron imaging experiments that we have done at OUAL over the past few years using our relatively simple prototype imaging detector have clearly demonstrated the potential effectiveness of high-energy neutron imaging and validated its proposed use as a nonintrusive inspection tool in DOE NDE applications. The engineering design of key components for our full-scale (10 MeV) neutron imaging system is essentially complete and a prototype facility operating with $E_n \sim 7$ MeV @ 0° should be ready for use in neutron source technology assessment and our next phase of imaging experiments at LLNL by early 2008.

ACKNOWLEDGMENTS

We would like to thank Drs. William McLean and Bryan Balazs at LLNL for their programmatic support and administrative guidance relating to this project, Dr. Andrew Anderson and Kipp Whittaker of LLNL for their support in running ALE3D calculations relevant to the development of the D_2 gas target endstation and Prof. David Ingram of Ohio University and the staff of OUAL for their support in facilitating neutron imaging experiments conducted there.

This work was performed at the University of California, Lawrence Livermore National Laboratory, under the auspices of the U.S. Department of Energy (contract # W-7405-Eng-48).

REFERENCES

[1] F. Dietrich and J. Hall, "Detector concept for neutron tomography in the 10 - 15 MeV energy range", UCRL-ID-123490 (LLNL, 1996).

[2] F. Dietrich, J. Hall and C. Logan, "Conceptual design for a neutron imaging system for thick target analysis operating in the 10 - 15 MeV energy range," UCRL-JC-124401 (LLNL, 1996), published in *14th Int. Conf. on the Application of Accelerators in Research and Industry* (Denton, TX, 1996), AIP **CP392**, ed. J. Duggan and I. Morgan, 837 (1997).

[3] J. Hall, F. Dietrich, C. Logan and G Schmid, "Development of high-energy neutron imaging for use in NDE applications", UCRL-JC-134562 (LLNL, 1999), published in *Penetrating Radiation Systems and Applications* (Denver, CO, 1999), SPIE **3769**, ed. F. Doty, 31 (1999).

[4] J. Hall, F. Dietrich, C. Logan and B. Rusnak, "Recent Results in the Development of Fast Neutron Imaging Techniques," UCRL-JC-140435 (LLNL, 2000), published in *16th Int. Conf. on the Application of Accelerators in Research and Industry* (Denton, TX, 2000), AIP **CP576**, ed. J. Duggan and I. Morgan, 1113 (2001).

[5] B. Rusnak and J. Hall, "An accelerator system for neutron radiography," UCRL-JC-139558 (LLNL, 2000), published in *16th Int. Conf. on the Applications of Accelerators in Research and Industry* (Denton, TX, 2000), AIP **CP576**, ed. J. Duggan and I. Morgan, 1105 (2001).

[6] J. Hall, "Uncovering hidden defects with neutrons," published in LLNL *Science & Technology Review*, May 2001 (LLNL, 2001).

[7] E. Iverson, R. Lanza and L. Lidsky, "Windowless gas targets for neutron production," published in *5th Int. Conf. on Neutrons in Research and Industry* (Crete, Greece, 1996), SPIE **2867**, ed. G. Vourvopoulos, 513 (1996).

[8] E. Iverson, "Windowless gas targets for neutron production," Ph.D. thesis, MIT, Cambridge, MA, February 1997; R. Lanza, MIT, private comm.

[9] W. Gerber, "Investigation of windowless gas target systems for particle accelerators," M.S. thesis, MIT, Cambridge, MA, June 1998; R. Lanza, MIT, private comm.

[10] E. Empey, "Implementation of a closed-loop windowless gas target system for neutron production," M.S. thesis, MIT, Cambridge, MA, February 2000; R. Lanza, MIT, private comm.

[11] J. Guzek, *et al.*, "Development of High-Pressure Deuterium Gas Targets for the Generation of Intense Monoenergetic Fast Neutron Beams," Nucl. Inst. & Meth. B **152**, 512 (1999).

[12] D. Schneberk, *et al.*, LLNL, private comm.